NANO LETTERS

2008
Vol. 8, No. 3
780-785

Quantum Dot Ex Vivo Labeling of Neuromuscular Synapses

Rebecca L. Orndorff,[†] Michael R. Warnement,[†] John N. Mason,[‡] Randy D. Blakely,[‡,||,⊥] and Sandra J. Rosenthal*[,†,‡,§]

Department of Chemistry, Vanderbilt University, Station B, 351822, Nashville, Tennessee 37235-1822, Department of Pharmacology, Vanderbilt School of Medicine, Vanderbilt University, Nashville, Tennessee 37235-1822, Department of Physics, Vanderbilt University, 1807 Station B, Nashville, Tennessee 37235-1822, Department of Psychiatry, Vanderbilt School of Medicine, Vanderbilt University, Nashville, Tennessee, 37235-1822, and Center for Molecular Neuroscience, Vanderbilt School of Medicine, Vanderbilt University, Nashville, Tennessee, 37235-1822

Received September 25, 2007; Revised Manuscript Received January 14, 2008

ABSTRACT

Nicotinic receptors (nAchRs) are responsible for fast excitatory signaling by the neurotransmitter acetylcholine (Ach). They are present on the postsynaptic membrane at neuromuscular junctions (NMJs) and also at brain synapses. α-Bungarotoxin (α-BTX), a high-affinity nAchR antagonist, inhibits Ach binding and neurotransmission.[1,2] Here we demonstrate biotinylated α-BTX, bound to native mouse diaphragm nAchRs, can be quantified and visualized ex vivo using streptavidin-conjugated quantum dots. This approach provides a novel methodology for the direct assessment of the presence and mobility of neurotransmitter receptors in native tissue.

Nicotinic acetylcholine receptors (nAchRs) are a well-studied class of ligand-gated ion channels. They are members of the ionotropic receptor Cys-loop superfamily[3] and are closely related to γ-amino butyric acid receptor type A ($GABA_A$) and glycine receptors; additionally, they are distant cousins to both serotonin (5HT-3) and glutamate (GluR) receptors. nAchRs are pentameric transmembrane proteins that consist of subunits surrounding a cation pore. Subunits are classified as α(1–10), β(1–5), δ, and γ (or ϵ in adult physiology) and found in both muscle tissues and neuronal tissues. Each subunit has high sequence identity with homologous subunits that combine to form an array of receptor subtypes throughout an organism. These receptors are further categorized as homopentamers or heteropentamers based upon their subunit organization.[2,4] In vertebrates, dense clusters of nAchRs are found in the *Torpedo* electric organ and in skeletal muscle such as diaphragm tissue.[5] The muscle type nAchRs are composed of an $\alpha_2\beta\gamma\delta$ stoichiometry of subunits. Together, these subunits create a cation pore through which ion flux[2] occurs after acetylcholine binding.

Antibody and toxin-labeling studies show that muscle-type nAchRs are clustered at the peaks of the highly folded postsynaptic muscle membrane. In the disorder myasthenia gravis (MG), nAchR antibodies induce a loss of these clusters, thereby producing muscle paralysis and, if untreated, death. Functioning nAchRs are also lost when targeted by certain neurotoxins such as α-bungarotoxin (α-BTX). α-BTX, a 74 amino acid peptide from the snake *Bungarus multicinctus*, has subnanomolar affinity for nAchRs and blocks neuromuscular transmission by preventing binding at the α-subunit interface with the δ and γ subunits.[2] Another venom component, β-bungarotoxin, acts presynaptically to trigger massive Ach release and subsequent depletion.[6] The α-BTX peptide has been used as a high-affinity ligand to label nAchRs for imaging and quantitation. Fluorescent and radiolabeled α-BTX conjugates are typically used;[7–11] however, biotinylation is also an option, as binding to target receptors can be detected with an avidin-linked probe.[11,12] Coupling of biotin and avidin, or streptavidin, yields an interaction with femtomolar affinity and a long half-life in solution. Common avidin probes include streptavidin−Alexafluor dye conjugates. Recent advances in probe development have generated streptavidin−quantum dot (streptavidin−QD) conjugates that may be even more suitable for

* Corresponding author. E-mail: sjr@femto.cas.Vanderbilt.edu. Telephone: +1 615 322 2633. Fax: + 1 615 343 1234.
† Department of Chemistry, Vanderbilt University.
‡ Department of Pharmacology, Vanderbilt School of Medicine, Vanderbilt University.
|| Department of Psychiatry, Vanderbilt School of Medicine, Vanderbilt University.
⊥ Center for Molecular Neuroscience, Vanderbilt School of Medicine, Vanderbilt University.
§ Department of Physics, Vanderbilt University.

10.1021/nl072460x CCC: $40.75
Published on Web 02/01/2008

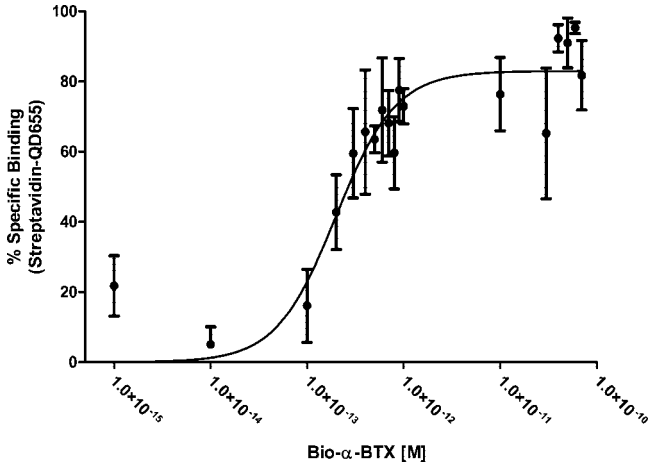

Figure 1. Bio-α-BTX saturation binding curve detected with streptavidin−QDs at NMJ synapses. Tissue was blocked and treated with dilutions of bio-α-BTX for 10 min and labeled with streptavidin−QD655s overnight at 4 °C. Data are the mean of three experiments ± SEM, with individual points assayed in triplicate for each experiment. K_D is 198 ± 43 fM; B_{max} is 89.93 ± 4.163%, and the Hill slope is 1.402 ± 0.3884. α-BTX binds nAchRs with subpicomolar affinity, approximately 1000-fold greater binding affinity than denatured nAchR assays.

biological applications given their multiplexing capabilities and resistance to photobleaching.[13–17]

Although both live and fixed cells have been labeled with QD conjugates, tissue labeling with QDs has been limited to fixed sections[17–25] and illumination tracking during surgical procedures.[26–31] We present QD labeling of nAchRs at NMJs in mature ex vivo mouse diaphragm. The neuroreceptors were targeted with the α-BTX conjugate, biotinylated α-BTX (bio-α-BTX), and used streptavidin−QD655s to visualize the bound bio-α-BTX in the whole mount tissue.

To examine α-BTX affinity in ex vivo tissue, mouse diaphragm was dissected and treated with glycine solution for one hour. The tissue was then incubated overnight in blocking solution at 4 °C. Following overnight blocking, the tissue was treated with blocking solution containing increasing concentrations of bio-α-BTX for approximately 10 min. Overnight incubation in blocking solution containing streptavidin−QD655s (Invitrogen, Inc.) occurred after toxin exposure. Tissue sections were mounted and imaged using invert confocal microscopy, LSM510 Meta (Zeiss, Inc.) Figure 1 illustrates the resulting saturation binding curve using the bio-α-BTX and streptavidin−QD655 labeling protocol. The observed bio-α-BTX affinity, K_D of approximately 200 fM, indicates that α-BTX has a much higher affinity for nAchRs at NMJ synapses than previously observed by Stephenson and co-workers.[1] This finding may indicate that receptors within ex vivo tissue retain higher affinity for the α-BTX antagonist than homogenized receptors extracted under denaturing conditions. The ability of α-BTX to bind nAchRs with subpicomolar affinity enables the antagonist to be used as a highly specific probe for QD labeling and imaging to study neuromuscular synapses.

To further analyze bio-α-BTX and streptavidin−QD655 efficacy as a probe for nAchRs, we performed time-dependence experiments with unfixed mouse diaphragms.

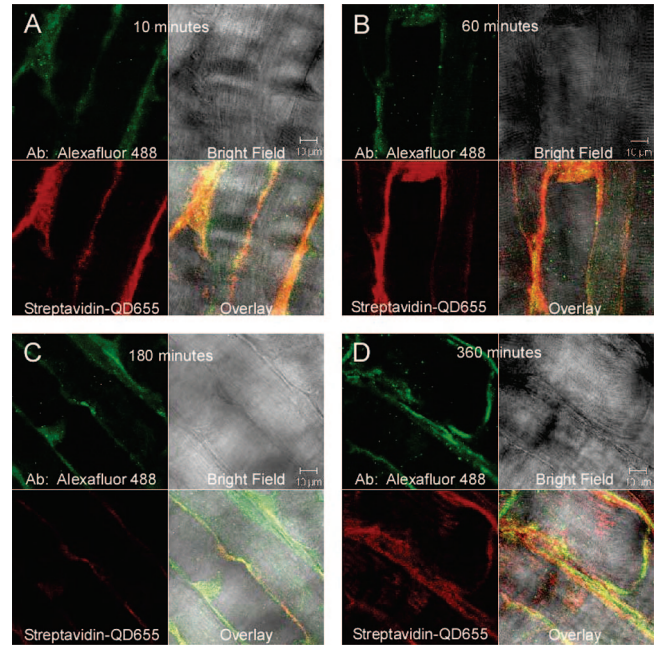

Figure 2. Time-dependence labeling of NMJs with bio-α-BTX after overnight blocking solution incubation. Images represent tissue incubated with 10 nM bio-α-BTX following blocking protocol and nAchRs detected with streptavidin−QD655 conjugates at (A) 10, (B) 60, (C) 180, and (D) 360 min. Experiments were run in triplicate with each piece imaged at least three times. α-BTX binding is detected in all sections and all time intervals with streptavidin−QD655s.

The first experiment was to determine whether length of bio-α-BTX exposure affected visualization with streptavidin−QD655 (Figures 2, 4A). We treated the tissue as previously described and exposed the tissue to bio-α-BTX for intervals of 10, 60, 180, 360 (Figure 2) and 720 (Figure 4A) min. Additionally, we coincubated the tissue with a nAchR β-antibody and secondary−Alexafluor488 antibody conjugate (Sigma, Inc.) to demonstrate probe specificity. A second experiment analyzed whether receptor viability remained in ex vivo tissue after seven days in blocking conditions prior to labeling with the bio-α-BTX and streptavidin−QD655 probe (Figure 3). Figure 2 illustrates that bio-α-BTX binds rapidly in fresh ex vivo tissue, where essentially full labeling was achieved at 10 min. Additionally, we observed that binding was highly specific, as demonstrated by colocalization between the streptavidin−QD655 fluorescence, labeling bio-α-BTX, and that of the Alexafluor488 antibody conjugate, labeling anti-nAchR subunit antibodies. This further substantiates the affinity determined in Figure 1, as noted by the lack of dissociation present at 720 min of exposure (Figure 4A). We also see that binding is equivalent between Figures 2 and 3 at each α-BTX incubation time. These data suggest that the nAchR remains viable over time when maintained in an ex vivo environment, which has potential relevance for production of sample archives for comparative analyses.

Next we performed analyses using streptavidin−Alexafluor555 (Invitrogen, Inc.) (Figure 4C,D) in place of streptavidin−QD655 (Figure 4A,B) to compare QD labeling efficacy versus a commonly used organic fluorophore.[10,32]

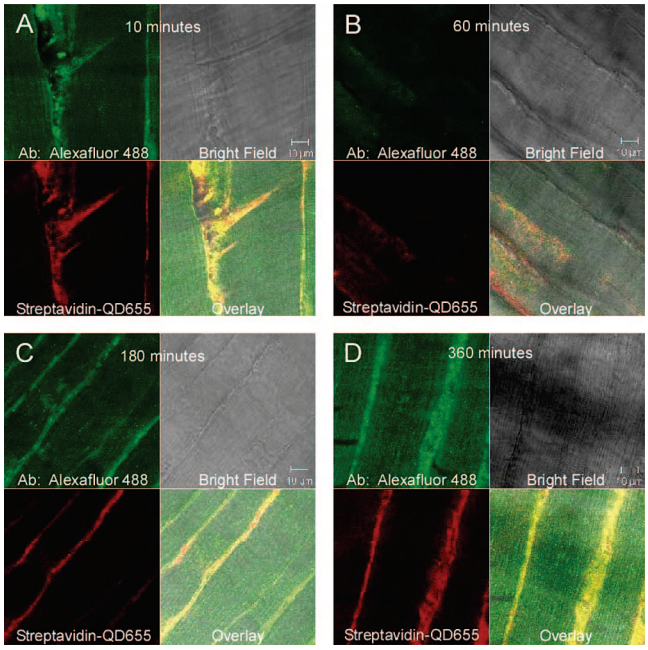

Figure 3. Time-dependence labeling of NMJs with bio-α-BTX after seven-day blocking solution incubation. Tissue was incubated with 10 nM bio-α-BTX and nAchRs were detected with streptavidin−QD655 conjugates at (A) 10, (B) 60, (C) 180, and (D) 360 min following seven-day blocking protocol. Each time interval was imaged at least three times. QD detection is unaffected by extended blocking solution incubation prior to α-BTX labeling.

Mouse diaphragms were exposed to bio-α-BTX for 720 min, and then labeled overnight in either streptavidin−QD655 or streptavidin−Alexafluor555 conjugates. Although both QDs and Alexafluors label NMJ synapses, imaging revealed that the QDs appear much brighter than their fluorophore counterparts. Quantitative analysis of the relative intensities of streptavidin−QD655 versus streptavidin−Alexafluor555 conjugates (Figure 4E,F) present statistically significant differences in intensity between the fluorescent probes ($0.001 < P < 0.01$, analysis of variance). The QDs exhibit a higher signal-to-noise ratio in tissue samples than fluorescent dyes and adequately label neural targets within an ex vivo system. This is particularly significant in that our experiments are reported at concentrations of bio-α-BTX that are 10 times lower than concentrations needed for Alexafluor labeling. To further verify the bio-α-BTX and streptavidin−QD655 labeling system utility, nAchR α-BTX binding sites were blocked with unconjugated α-BTX using a concentration of α-BTX 10 times in excess of the bio-α-BTX used for detecting the NMJ nAchRs. Figure 5 illustrates that labeling at the α-BTX site is blocked by the presence of α-BTX prior to introduction of the biotinylated conjugate. These findings also indicate that bio-α-BTX does not displace α-BTX within the exposure period and that the labeling is specific to the α-BTX binding site (BBS) sequence, a 13-aa sequence found on the α-subunit of the nAchR.[8,11,33]

An additional assessment of the bio-α-BTX and streptavidin−QD655 probe examined QD photostability relative to the Alexafluor dyes. Resistance to photobleaching is a known characteristic of QDs.[7–10] Figure 6A1–A5 demonstrate photobleaching resistance of QDs versus the secondary antibody

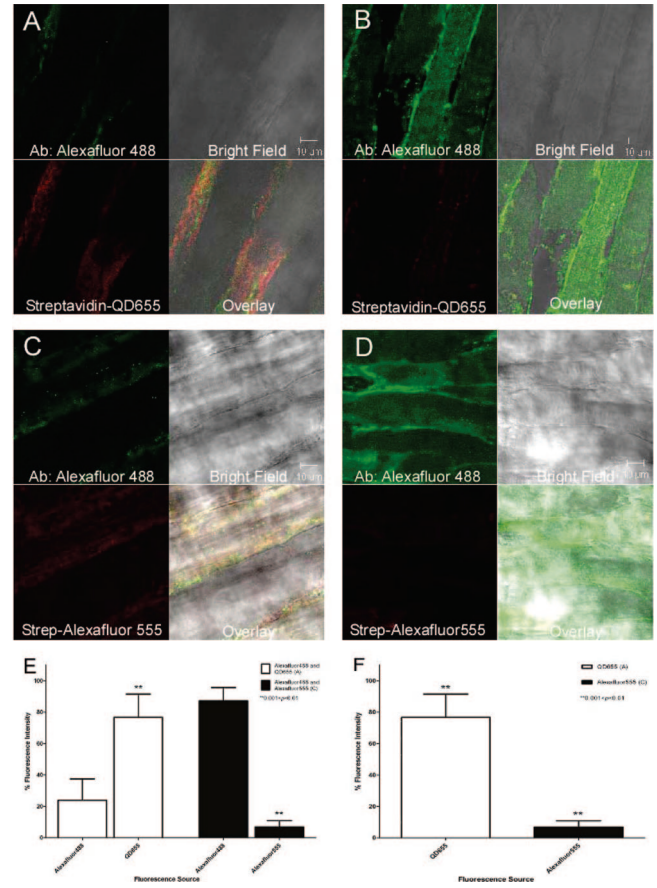

Figure 4. Comparative analyses between streptavidin−QD655s and streptavidin−Alexafluor555s detection of bio-α-BTX at NMJ synapses. All tissue was blocked and exposed to 10 nM bio-α-BTX, or blocking solution, for 12 h, and treated with streptavidin−QD655 or Alexafluor555 conjugates overnight at 4 °C. Images represent a compilation of three experiments. (A,C) 12 h 10 nM bio-α-BTX and primary antibody incubation. (B,D) Controls incubated in blocking solution with primary antibody only. nAchRs detected with 10 nM fluorescent probe (A) streptavidin−QD655, (C) streptavidin−Alexafluor555. Alexafluor488 colocalization (A,C) with streptavidin−QD655s (A) and streptavidin−Alexafluor555s (C) indicates effective labeling of nAchRs. Absence of bio-α-BTX (B,D) results in a lack of labeling by both streptavidin−QD655s (B) and streptavidin−Alexafluor555s (D). Relative fluorescence intensity (E,F) reveals statistical significance between streptavidin−QD655 and streptavidin−Alexafluor555 fluorescence ($0.001 < P < 0.01$, analysis of variance, values are the means ± SEM).

Alexafluor488 conjugate (Figure 6A1–A5) and relative to streptavidin−Alexafluor555s (Figure 6B1–B5) within ex vivo tissue. The tissue was imaged using an LSM510 Meta inverted confocal microscope (Zeiss, Inc.) and exposed to continuous excitation for approximately 30 min. As time progressed, the Alexafluor conjugates, Alexafluor488 and Alexafluor555, photobleached rapidly in ex vivo tissue under continuous excitation. QDs, however, retained their photostability throughout continuous excitation, as illustrated in Figure 6A1–A5. There is significant reduction in Alexafluor488 intensity at 180 s and no reduction in QD intensity at the same time interval (Figure 6A2). After 720 s of continuous fluorescence excitation in tissue, QDs maintain their brightness, whereas Alexafluor488 is effectively pho-

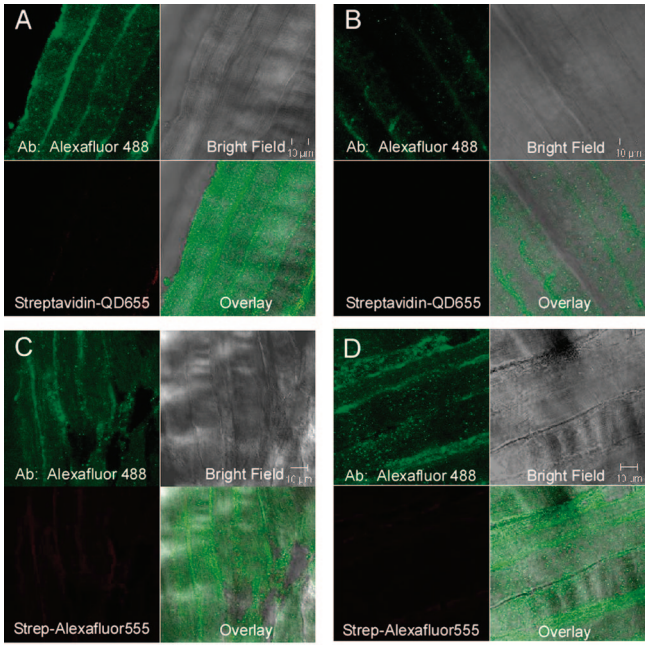

Figure 5. NMJ synapses pretreated with 100 nM α-BTX exhibit neither streptavidin−QD655 nor streptavidin−Alexafluor555 labeling after 10 nM bio-α-BTX incubation. Tissue was incubated with 100 nM α-BTX overnight, then treated with 10 nM bio-α-BTX for 12 h. Images are representative of three experiments. Presence of bio-α-BTX labeling was not detected after streptavidin−QD655 and Alexafluor555 treatment overnight. Alexafluor488 labeling at the nAchR β-subunit is unaffected by α-BTX pretreatment. This indicates that both streptavidin−QD655 and streptavidin−Alexafluor555 labeling is specific to the BBS.

tobleached. Figure 6C further supports that QDs lose minimal intensity over time during repeated excitation. We measured photobleaching resistance for both fluorophores and QDs relative to fluorescein isothiocyanate (FITC) by spin-casting (a solvent evaporation technique that deposits fluorescent probes directly onto a spinning surface) each fluorescent probe and exposing the cast to continuous excitation on a Zeiss Axiovert 200 M inverted widefield microscope (Zeiss, Inc.) with Metamorph (MDS, Inc.) for 30 min. The trends in Figure 6C affirm the photobleaching data obtained using the mouse diaphragms and suggest that QDs are a suitable fluorescent probe for targeting neuroreceptors in ex vivo tissue.

Saturation binding analysis revealed that α-BTX has 1000-fold higher affinity for native nAchRs than previously reported.[1] This indicates that it is a highly specific ligand that may be used in conjunction with a recombinant BBS to study neural targets lacking suitable high-affinity probes.[8,11] Bio-α-BTX was shown to maintain high affinity for nAchRs over time. α-BTX also blocked nAchR detection by bio-α-BTX when exposed to muscle tissue. Our findings additionally indicate that streptavidin−QD655s are photostable fluorescent probes suitable for detecting nAchRs in ex vivo tissue using bio-α-BTX.

QDs exhibit traits that are not seen with organic fluorophores, such as near 100% quantum yield.[34] Their incorporation into biological experiments has required surface modification for biocompatibility. Reduction of nonspecific binding to cell membranes have included modifications such as micelle encapsulation,[35] pegilation,[36] selinization,[37] coating in amphiphilic polymers,[38,39] and addition of biologically active molecules such as proteins,[17,40,41] peptides,[42–44] small molecules,[45–47] and antibodies[48–51] to the surface of the QDs. Results of these surface modifications to QDs have included successes in cell culture labeling.[17–21,26,36,52–58] The Ting laboratory recently reported use of streptavidin−QD conjugates through biotin ligase biotinylation of tagged cyan fluorescent protein and epidermal growth factor receptors in HeLa cell cultures and α-amino-3-hydroxy-5-methyl-4-isoxazolepropionate (AMPA) receptors in neurons.[43] Their results demonstrated the utility of biotin−streptavidin QD coupling for targeting neuroreceptors and neurons. Our findings further support biological suitability and provide evidence for QD use in other tissues and neural targets.

Biological applications for QDs include live cell-trafficking assays for neural target studies, which require high probe specificity and photostability within unfixed conditions. Preliminary evidence demonstrates suitability of this approach for labeling nAchRs in the brain following ICV injection of bio-α-BTX (Orndorff and Rosenthal, unpublished findings). Furthermore, our results demonstrate ex vivo labeling efficacy of neuromuscular synapses with QDs.

Methods and Materials. All experiments were performed using C57BL/6 inbred mice between 8 and 10 weeks of age and sacrificed in accordance to IACUC standards and procedure protocols.

Labeling Assays. ***Blocking Protocol.*** Dissected mouse diaphragm was obtained and washed in 1× phosphate-buffered saline (PBS) solution for approximately 1 h on ice. The tissue was then divided into equal portions and incubated in 100 mM glycine in 1× PBS (pH 7.3) for 1 h on ice. Overnight incubation at 4 °C followed in blocking solution consisting of 1× PBS (pH 7.3), 5% normal goat serum, 3% bovine serum albumin, 0.2% Triton X-100, and 0.01% thimerosal.

The tissue was then briefly washed in 1× PBS solution. Mouse diaphragm sections were exposed to α-BTX for the experimental time interval (10, 60, 180, 360, or 720 min) incubation at 4 °C in blocking solution consisting of 1× PBS (pH 7.3), 5% normal goat serum, 3% bovine serum albumin, 0.01% thimerosal, nAchR β-subunit rat-anti-nAchR primary antibody (1:5000) (Sigma, Inc.), and 10 nM bio-α-BTX (Invitrogen, Inc.); the control sections were exposed to the same conditions without the bio-α-BTX.

The tissue sections were briefly washed in 1× PBS solution. Overnight incubation at 4 °C followed with Alexafluor488−rabbit-antirat secondary antibody conjugate (1:5000) 10 nM streptavidin−QD655 conjugates in blocking solution. The procedure was repeated in parallel with 10 nM streptavidin−Alexafluor555 conjugates in blocking solution with the remaining tissue sections. The tissue sections were then washed in 1× PBS three times for 10 min on ice and mounted using AquaMount antiphotobleaching solution for

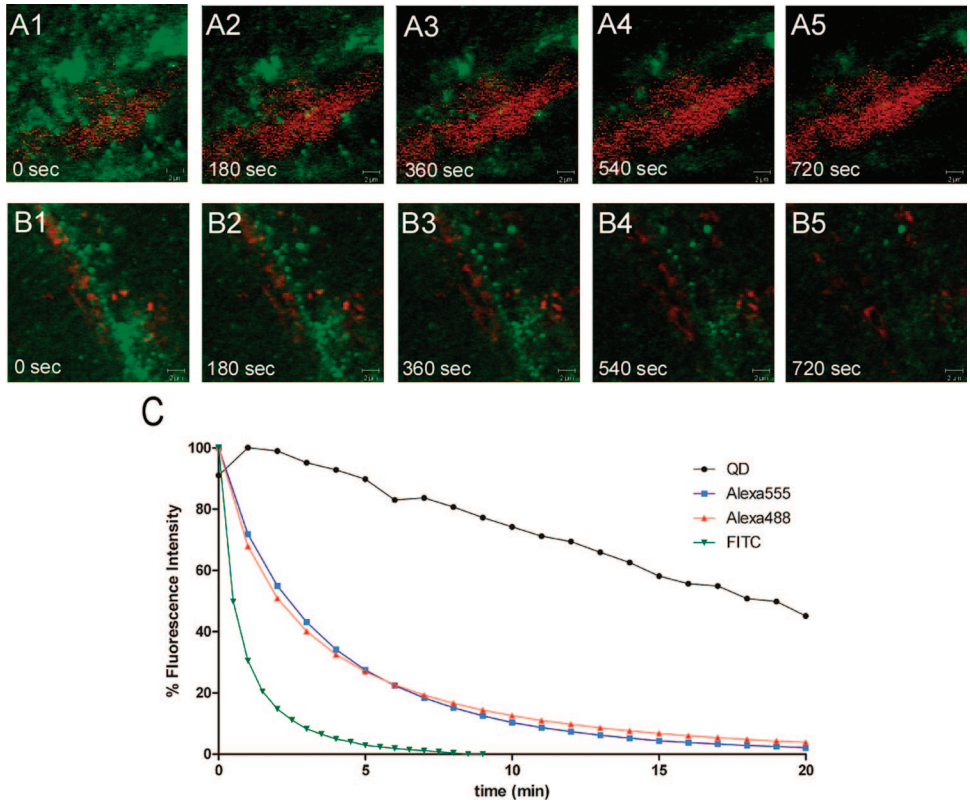

Figure 6. Photostability of QDs vs Alexafluor dyes in tissue and by spin-casting. The samples were treated with 10 nM bio-α-BTX and *β*-antibody (1:5000) for 10 min. Tissue samples were then incubated with secondary−Alexafluor488 antibody and either streptavidin−QD655s (A1−A5) or streptavidin−Alexafluor555s (B1−B5) overnight. Images were captured during continuous excitation of fluorescent probes using an inverted confocal microscope for 30 min. At approximately 180 s (A2,B2), there is significant photobleaching present in both Alexafluor488 and Alexafluor555 and no photobleaching present in QD655s. By 720 s (A5,B5), both Alexafluor dyes are photobleached and QDs maintain their initial intensity. (C) Continuous excitation for 30 min using Zeiss Axiovert 200 M wide-field microscope with Metamorph imaging software of spin-cast, fluorescent probe deposition onto spinning surface for solvent evaporation, streptavidin−QD655s, streptavidin−Alexafluor555s, and secondary−Alexafluor488 antibody conjugate vs FITC. Alexafluor dyes photobleach after less than 10 min of continuous excitation, and QDs are photostable after more than 30 min of continuous excitation, regardless of medium.

imaging. The labeling protocol was repeated for 10, 60, 180, and 360 min with tissue that was incubated in blocking solution at 4 °C for seven days.

α-Bungarotoxin Affinity Assay. Saturation binding curves were generated using dissected tissue, treated as previously described, and incubated with dilutions of bio-α-BTX for 10 min at 4 °C. The tissue sections were incubated overnight in 10 nM streptavidin−QD655s, washed 3× for 10 min, and mounted with AquaMount. Mouse diaphragm sections were additionally exposed to 100 nM α-BTX in blocking solution overnight (approximately 12 h) at 4 °C as pretreatment to determine affinity. Tissue was treated as before with 10 nM bio-α-BTX and primary antibody (1:5000) and labeled with streptavidin−QD655 and streptavidin−Alexafluor555. All tissue was imaged using an inverted confocal microscope (Zeiss, Inc.) and analyzed using Metamorph software (MDS, Inc.). Data was analyzed and saturation binding curves were generated using Prism (GraphPad Prism Software, Inc.).

Photobleaching Assays. Samples were prepared as before, with exposure to bio-α-BTX for 10 min. The samples were mounted without AquaMount. Following sample preparations, each was imaged as before. Each conjugate was also spin-cast, dropped onto a spinning surface for solvent evaporation, and imaged using a Zeiss Axiovert 200 M wide-field microscope with Metamorph. FITC was run as a standard.

Acknowledgment. We are grateful for the support and insight provided by the Blakely Laboratory, specifically Jane Wright, David Lund, and Dr. Alicia Ruggiero. We would also like to thank Dr. Heinrich J. G. Matthies for providing the tissue necessary for applications within the brain and the laboratory of Dr. Ronald G. Wiley. Additionally, we would like to thank Sean Schaffer of the Vanderbilt Cell Imaging Shared Resource Core for the microscopy training received. The Vanderbilt University Vivarium faculty and staff are also acknowledged. This work was supported by National Institutes of Health grant RO1 601504204301381 and P20 GM7204802.

References

(1) Stephenson, F. A.; Harrison, R.; Lunt, G. G. *Eur. J. Biochem., FEBS* **1981**, *115*, 91–97.
(2) Arias, H. R. *Neurochem. Int.* **2000**, *36*, 595–645.
(3) Sine, S. M.; Engel, A. G. *Nature* **2006**, *440*, 448–455.
(4) Gotti, C.; Clementi, F. *Prog. Neurobiol.* **2004**, *74*, 363–396.
(5) Connolly, J. G. *Comp. Biochem. Physiol., Part A: Mol. Integr. Physiol.* **1989**, *93*, 221–231.
(6) Chang, C. C. *J. Biomed. Sci* **1999**, *6*, 368–375.
(7) Clark, P. B. S.; Schwartz, R. D.; Paul, S. M.; Pert, C. B.; Pert, A. *J. Neurosci.* **1985**, *5*, 1307–1315.

(8) Bogdanov, Y.; Michels, G.; Armstrong-Gold, C.; Haydon, P. G.; Lindstrom, J.; Pangalos, M.; Moss, S. J. *EMBO J.* **2006**, *25*, 4381–4389.
(9) Gottschalk, A.; Schafer, W. R. *J. Neurosci. Methods* **2006**, *154*, 68–79.
(10) Ferguson, S. M.; Bazalakova, M.; Savchenko, V.; Tapia, J. C.; Wright, J.; Blakely, R. D. *Proc. Natl. Acad. Sci. U.S.A.* **2004**, *101*, 8762–8767.
(11) Sekine-Aizawa, Y.; Huganir, R. L. *Proc. Natl. Acad. Sci. U.S.A.* **2004**, *101*, 17114–17119.
(12) Bruneau, E.; Sutter, D.; Hume, R. I.; Akaaboune, M. *J. Neurosci.* **2005**, *25*, 9949–9959.
(13) Peng, Z. A.; Peng, X. *J. Am. Chem. Soc.* **2001**, *123*, 183–184.
(14) Michalet, X.; Pinaud, F.; Lacoste, T. D.; Dahan, M.; Bruchez, M. P.; Alivisatos, A. P.; Weiss, S. *Single Mol.* **2001**, *2*, 261–276.
(15) Bruchez, M.; Moronne, M.; Gin, P.; Weiss, S.; Alivisatos, A. P. *Science* **1998**, *281*, 2013–2016.
(16) Chan, W. C. W.; Nie, S. *Science* **1998**, *281*, 2016–2018.
(17) Wu, X.; Liu, H.; Liu, J.; Haley, K. N.; Treadway, J. A.; Larson, J. P.; Ge, N.; Peale, F.; Bruchez, M., P. *Nat. Biotechnol.* **2002**, *21*, 41–46.
(18) Hoshino, A.; Hanaki, K.; Suzuki, K.; Yamamoto, K. *Biochem. Biophys. Res. Commun.* **2004**, *314*, 46–53.
(19) Estrada, C. R.; Salanga, M.; Bielenberg, D. R.; Harrell, W. B.; Zurakowski, D.; Zhu, X.; Palmer, M. R.; Freeman, M. R.; Adam, R. M. *Cancer Res.* **2006**, *66*, 3078–3086.
(20) Chu, T. C.; Shieh, F.; Lavery, L. A.; Levy, M.; Richards-Kortum, R.; Korgel, B. A.; Ellington, A. D. *Biosens. Bioelectron.* **2006**, *21*, 1859–1866.
(21) Giepmans, B. N. G.; Deerinck, T. J.; Smarr, B. L.; Jones, Y. Z.; Ellisman, M. H. *Nat. Methods* **2005**, *2*, 743–749.
(22) Fountaine, T. J.; Wincovitch, S. M.; Geho, D. H.; Gargield, S. H.; Pittaluga, S. *Mod. Pathol.* **2006**, *19*, 1181–1191.
(23) Tholouli, E.; Hoyland, J. A.; Di Vizio, D.; O'Connell, F.; MacDermott, S. A.; Twomey, D.; Levenson, R.; Liu Yin, J. A.; Golub, T. R.; Loda, M.; Byers, R. *Biochem. Biophys. Res. Commun.* **2006**, *348*, 628–636.
(24) Chan, P.; Yuen, T.; Ruf, F.; Gonzalez-Maeso, J.; Sealfon, S. C. *Nucleic Acids Res.* **2005**, *33*, e161–e169.
(25) Ferrara, D. E.; Weiss, D.; Carnell, P. H.; Vito, R. P.; Vega, D.; Gao, X.; Nie, S.; Taylor, W. R. *Am. J. Physiol.: Regul. Integr. Comp. Physiol.* **2006**, *290*, 114–123.
(26) Voura, E. B.; Haiswal, J. K.; Mattoussi, H.; Simon, S. M. *Nat. Med.* **2004**, *10*, 993–998.
(27) Levene, M. J.; Dombeck, D. A.; Kasischke, K. A.; Molloy, R. P.; Webb, W. W. *J. Neurophysiol.* **2004**, *91*, 1908–1912.
(28) Kim, S.; Lim, Y. T.; Soltesz, E. G.; De Grand, A. M.; Lee, J.; Nakayama, A.; Anthony, P. J.; Mihaljevic, T.; Laurence, R. G.; Dor, D. M.; Cohn, L. H.; Bawendi, M. G.; Frangioni, J. V. *Nat. Biotechnol.* **2004**, *22*, 93–97.
(29) Soltesz, E. G.; Kim, S.; Laurence, R. G.; DeGrand, A. M.; Parungo, C. P.; Dor, D. M.; Cohn, L. H.; Bawendi, M. G.; Frangioni, J. V.; Mihaljevic, T. *Ann. Thorac. Surg.* **2005**, *79*, 269–277.
(30) Soltesz, E. G.; Kim, S.; Kim, S.-W.; Laurence, R. G.; De Grand, A. M.; Parungo, C. P.; Cohn, L. H.; Bawendi, M. G.; Frangioni, J. V. *Ann. Surg. Oncol.* **2006**, *13*, 386–396.
(31) Larson, D. R.; Zipfel, W. R.; Williams, R. M.; Clark, S. W.; Bruchez, M. P.; Wise, F. W.; Webb, W. W. *Science* **2003**, *300*, 1434–1436.
(32) Misgeld, T.; Burgess, R. W.; Lewis, R. M.; Cunningham, J. M.; Lechtman, J. W.; Sanes, J. R. *Neuron* **2002**, *36*, 635–648.
(33) Harel, M.; Kasher, R.; Nicolas, A.; Guss, J. M.; Balass, M.; Fridkin, M.; Smit, A. B.; Brejc, K.; Sixma, T. K.; Katchalski-Katzir, E.; Sussman, J. L.; Fuchs, S. *Neuron* **2001**, *32*, 265–275.
(34) McBride, J.; Treadway, J.; Feldman, L. C.; Pennycook, S. J.; Rosenthal, S. J. *Nano Lett.* **2006**, *6*, 1496–1501.
(35) Dubertret, B.; Skourides, P.; Norris, D. J.; Noireaux, V.; Brivanlou, A. H.; Libchaber, A. *Science* **2002**, *298*, 1759–1762.
(36) Bentzen, E. L.; Tomlinson, I. D.; Mason, J.; Gresch, P.; Warnement, M. R.; Wright, D.; Sanders-Bush, E.; Blakely, R.; Rosenthal, S. J. *Bioconjugate Chem.* **2005**, *16*, 1488–1494.
(37) Gerion, D.; Pinaud, F.; Williams, S. C.; Parak, W. J.; Weiss, S.; Alivisatos, A. P. *J. Phys. Chem. B* **2001**, *105*, 8861–8871.
(38) Gao, X. H.; Cui, Y. Y.; Levenson, R. M.; Chung, L. W. K.; Nie, S. M. *Nat. Biotechnol.* **2004**, *22*, 969–976.
(39) Jovin, T. M. *Nat. Biotechnol.* **2003**, *21*, 32–33.
(40) Chun-Yang, Z.; Yi-Xuan, G.; Hui, M.; Cheng-Cai, A.; Die-Yan, C. *Analyst* **2000**, *125*, 1539–1542.
(41) Minet, O.; Dressler, C.; Beuthan, J. *J. Fluoresc.* **2004**, *14*, 241–247.
(42) Tomlinson, I. D., Mason, J. N., Blakely, R. D., Rosenthal, S. J., Peptide-conjugated quantum dots: Imaging the angiotensin type 1 receptor in living cells. In *Nanobiotechnology Protocols*; Methods In Molecular Biology, Vol. 303; Rosenthal, S. J. , Wright, D. W. , Eds.; Humana Press, Inc.: Totowa, NJ, 2005; pp 51–60..
(43) Lidke, D. S.; Nagy, P.; Heintzmann, R.; Arndt-Jovin, D. J.; Post, J. N.; Grecco, H. E.; Jares-Erijman, E. A.; Jovin, T. M. *Nat. Biotechnol.* **2004**, *22*, 198–203.
(44) Åkerman, M. E.; Chan, W. C. W.; Laakkonen, P.; Bhatia, S. N.; Ruoslahti, E. *Proc. Natl. Acad. Sci. U.S.A.* **2002**, *99*, 12617–12621.
(45) Gussin, H. A.; Tomlinson, I. D.; Little, D. M.; Warnement, M. R.; Qian, H.; Rosenthal, S. J.; Pepperberg, D. R. *J. Am. Chem. Soc.* **2006**, *128*, 15701–15713.
(46) Rosenthal, S. J.; Tomlinson, A.; Adkins, E. M.; Schroeter, S.; Adams, S.; Swafford, L.; McBride, J.; Wang, Y. Q.; DeFelice, L. J.; Blakely, R. D. *J. Am. Chem. Soc.* **2002**, *124*, 4586–4594.
(47) Tomlinson, I. D.; Mason, J. N.; Blakely, R. D.; Rosenthal, S. J. *Bioorg. Med. Chem. Lett.* **2006**, *16*, 4664–4667.
(48) Ballou, B.; Lagerholm, B. C.; Ernst, L. A.; Bruchez, M. P.; Waggoner, A. S. *Bioconjugate Chem.* **2004**, *15*, 79–86.
(49) Dahan, M.; Levi, S.; Luccardini, C.; Rostaing, P.; Riveau, B.; Triller, A. *Science* **2003**, *302*, 442–445.
(50) Goldman, E. R.; Clapp, A. R.; Anderson, G. P.; Uyeda, H. T.; Mauro, J. M.; Medintz, I. L.; Mattoussi, H. *Anal. Chem.* **2004**, *76*, 684–688.
(51) Mason, J. N.; Farmer, H.; Tomlinson, I. D.; Schwartz, J. W.; Savchenko, V.; DeFelice, L. J.; Rosenthal, S. J.; Blakely, R. D. *J. Neurosci. Methods* **2005**, *143*, 3–25.
(52) Osaki, F.; Kanamori, T.; Sando, S.; Sera, T.; Aoyama, Y. *J. Am. Chem. Soc.* **2004**, *126*, 6520–6521.
(53) Parak, W. J.; Boudreau, R.; Le Gros, M.; Gerion, D.; Zanchet, D.; Micheel, C. M.; Williams, S. C.; Alivisatos, A. P.; Larabell, C. *Adv. Mater.* **2002**, *14*, 882–885.
(54) Gomez, N.; Winter, J. O.; Shieh, F.; Saunders, A. E.; Korgel, B. A.; Schmidt, C. E. *Talanta* **2005**, *67*, 462–471.
(55) Hanaki, K.; Momo, A.; Oku, T.; Komoto, A.; Mainosono, S.; Yanaguchi, Y.; Yamamoto, K. *Biochem. Biophys. Res. Commun.* **2003**, *302*, 496–501.
(56) Sukhanova, A.; Devy, J.; Venteo, L.; Kaplan, H.; Artemyev, M.; Oleinikov, V.; Klinov, D.; Pluot, M.; Cohen, J. H. M.; Nabiev, I. *Anal. Biochem.* **2004**, *324*, 60–67.
(57) Clarke, S. J.; Hollmann, C. A.; Zhang, Z.; Suffern, D.; Bradforth, S. E.; Dimitrijevic, N. M.; Minarik, W. G.; Nadeau, J. L. *Nat. Mater.* **2006**, *5*, 409–417.
(58) Howarth, M.; Takao, K.; Hayashi, Y.; Ting, A. Y. *Proc. Natl. Acad. Sci. U.S.A.* **2005**, *102*, 7583–7588.

NL072460X